AUT Journal of Civil Engineering

AUT J. Civil Eng., 2(1) (2018) 103-114
DOI: 10.22060/ajce.2017.12425.5213

Theoretical and Experimental Study on Steel Plate Shear Wall with Unequal Columns

P. Mousavi Qieh-Qeshlaghi, S. Sabouri-Ghomi

Civil Engineering Department, K.N.Toosi University of Technology, Tehran, Iran

ABSTRACT: Steel plate shear walls with openings are highly interested because of their architectural aspects. A particular type of these systems is the steel plate shear wall with a door-shaped opening; the opening is continued from the base to top beam and surrounded by vertical boundary elements relatively weaker to main columns. Assuming the pure shear behavior for this system, each of the side panels can be considered a steel plate shear wall with unequal VBEs (vertical boundary elements). Behavior of this type of steel shear walls cannot be predicted by the common relations of steel shear walls; therefore, it has not been covered in technical literature until now. In this study, the behavior of steel plate shear wall with one strong and one weak column is theoretically and experimentally investigated. Theoretical relations to define the load-displacement curve and the inclination angle of tension field are proposed. An experimental model of a steel shear wall with unequal columns is fabricated and tested under cyclic quasi-static loading. Results of the experimental tests including load-displacement curve, plastic hinges location and inclination angle of tension field are compared with theoretical results.

Review History:

Received: 17 January 2017
Revised: 15 February 2017
Accepted: 2 March 2017
Available Online: 10 March 2018

Keywords:
Steel Plate Shear Walls
Door Type Opening
Unequal Columns
Plate-frame Interaction Theory
Tension Field Action

1- Introduction

Steel plate shear walls are known as an efficient and effective lateral load resisting system. For the past few decades, interest has developed in Steel Plate Shear Walls (SPSWs) as a structural lateral load resisting system for buildings [1]. Because of the dissipation of a large amount of energy, steel plate shear walls can be beneficial in highly active seismic zones [2]. One of the advantages of steel shear walls is the providing of openings in the infill plate, which sometimes are required for architectural reasons [3]. These openings can be applied in various sizes and shapes at any point of the shear wall. Examples of steel shear walls with common openings are shown in Figure 1. Door-shaped openings are one of the usual opening types that are continued along the wall height. From the economic and aesthetic points of view, the boundary elements on sides of the opening are not as the same as the main columns. Consequently, each of the shear panels on sides of the opening behaves as a shear wall with unequal boundary elements (unequal columns). Figure 2 shows the schematics of an SPSW with unequal columns that are a side panel of an SPSW with a door-shaped opening. This research performs to study the behavior of one of the side panels of a steel plate shear wall named as a steel plate shear wall with unequal columns.

The primary investigation on shear plates has been carried out by Wagner [4]. Based on the tests conducted on aluminum thin shear panels, he proposed the theory of diagonal tension field. Afterward, many investigators such as Busler [5] and Porter [6] studied the strength of diagonal tension field in plate girders. Takahashi et al. [7] conducted experimental research on the behavior of SPSW with door type opening. Obtained result showed

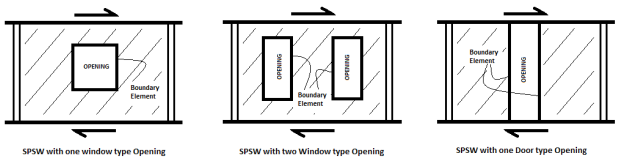

Figure 1. Common types of openings in steel shear walls

that the stiffness and ultimate shear strength of the SPSW are supplied well with keeping adequate reinforcement around it. It can be said that the first analytical study on SPSWs without stiffeners has been carried out by Thorburn et al. [8].

Corresponding author, E-mail: mousavi@dena.kntu.ac.ir

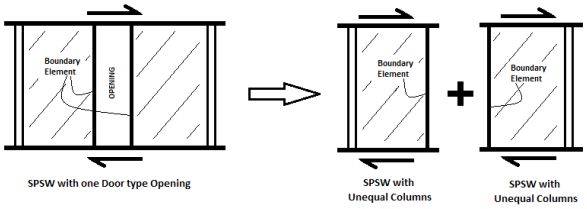

Figure 2. An SPSW with door-type opening and its equality as two SPSWs with unequal column

By considering the significant effect of infill plate tension in the ultimate behavior of the system, they proposed an analytical model, named strip model, for simulation of tension, filed behavior in a plate. They also developed a formula to predict the inclination angle of tension field based on the principle of least work done by plate and surrounding frame. The proposed formulation considers only the axial behavior of the plate, beam, and columns. In order to substantiate the proposed analytical method of Thorburn, et al. an experimental program has been conducted by Timler and kulak [9]. They revealed that the proportion of column flexural behavior should be also considered in determination of tension field angle. Sabouri-ghommi and Roberts [10] proposed a comprehensive theory named as Plate-Frame Interaction theory for predicting the behavior of steel plate shear walls in different configurations including thin or thick plate, with or without opening and stiffeners. This theory describes the behavior of a steel plate shear wall by summing the behavior of its components including plate and frame separately [11, 12]. Roberts and Sabouri-ghommi [13] conducted cyclic loading tests on un-stiffened steel shear panels with centrally placed circular opening. They concluded that the shear strength and initial stiffness of a perforated panel can be achieved by applying a modification factor to shear strength and initial stiffness a similar solid panel. Berman and Bruneau [14] developed analytical formulations for determining shear strength of steel shear wall based on strip models.

Vian and Bruneau [15] conducted experimental study on perforated steel shear walls and in continuing analytical studies on perforated steel shear walls by Paik [16] and Purba and Bruneau [17] were developed. Choi and Park [18] preformed experimental study on steel plate shear walls with various configurations of infill plates including steel shear wall with no connection of plate to side columns named as partially connected infill plate and steel shear wall with door type opening named as coupled steel shear wall. In their studies, the concept of effective tension field describing the concept of participated and non-participated area in tension field action was introduced. They also proposed the theoretical relations to define the inclination angle of tension field and shear capacity for the partially connected steel shear wall. Sabouri-ghommi and sadjadi [19, 20] conducted experimental study on steel shear walls with and without stiffeners. They also investigated the effect of opening on reduction of initial stiffness and ultimate strength of the system. In continuing Hoseinzadeh, et al. [21] and Valizadeh, et al. [2] performed studies on the effect of openings in the behavior of steel shear walls. Sabouri-ghommi and Mamazizi [3] studied experimentally on the effect of two openings with different distance from each other on the structural behavior of SPSWs. In their research, also the behavior of the area between to openings has been investigated. Purba and Bruneau [23] conducted experimental study on the effect of in-span plastic hinges in horizontal boundary elements on the seismic behavior of steel plate shear wall. Wang, et al. [24] performed numerical studies on the different infill plate configurations of steel shear walls including unstiffened plate, cross stiffened plate, infill plate with vertical slits, regularly perforated infill plate, low yield point infill plate, diagonal stiffened infill plate, slotted at side edges infill plate and steel shear wall with door type opening in one side.

In this study the behavior of steel plate shear wall with one strong and weak column is investigated theoretically and experimentally. Theoretical relations to define the load-displacement curve by considering the separate action of plate, strong column and weak column and also a relation to define the inclination angle of tension field are proposed. An experimental model of a steel shear wall with unequal VBE (vertical boundary elements) is fabricated and tested under cyclic quasi-static loading. Results of the experimental tests including load-displacement curve, plastic hinges location and inclination angle of tension field is compared with theoretical results. In order to fully study of theoretical relations, 12 numerical models with different overall dimension and column cross sections are investigated in finite element method and the probable errors in results are analyzed. The obtained results showed good agreement between theoretical relations and real behavior of this system and applicability of the relations in design of them.

2- Analytical relations

2- 1- Basic concepts

When a lateral load deforms the framing, the infill plate starts to develop a tension field after the onset of global buckling, and the inward force induced by the tension field action is resisted by the bending rigidity of the boundary elements [25]. The boundary elements, especially the vertical boundary elements (VBEs) require sufficient stiffness and strength to ensure the extensive yielding of the infill panel [25]. In this case, the tension field is uniformly distributed across the infill plate. On the other hand, when one of the vertical boundary elements has not sufficient strength and stiffness, it cannot resist the tension field force of the infill plate; therefore, parts of the infill plate beside the weak column cannot ensure the extensive yielding; in brief, the tension field is partially distributed across the infill plate [18]. In this case, two areas are formed in shear plate. In one of the area, the tension field action is induced and it is called as "participating area".

In the other area, the tension field action is not formed and thus, it is named as "non-participating area". In this situation, the location of plastic hinges in weak VBE is different from common SPSW with uniformly distributed tension field. By increasing the lateral displacement of the system, two plastic hinges are formed in the top and bottom of the strong column; then the other two plastic hinges are formed on the weak VBE in the beginning and end of the participation zone of tension field action. Therefore, it can be said that one of the plastic hinges is formed in the top or bottom of the weak column and

another plastic hinge is formed at a location along the weak column named as "in span plastic hinge". Also in this way, the inclination angle of tension field is also different from common SPSW proposed by Timler and Kulak [9]. Figure 3 shows the borders of participating and none-participating areas and position of plastic hinges in VBEs and tension filed in SPSWs with unequal columns.

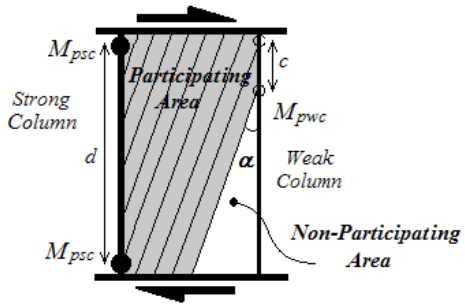

Figure 3. SPSW with unequal columns and formation of plastic hinges in VBEs and tension field in shear panel

2- 2- Structural capacity

The relations proposed in this study are based on Plate-Frame Interaction theory developed by Roberts and Sabouri [10]. In this method, shear capacity of the system is calculated separately considering the capacity of infill plate, strong column and weak column. In deriving relations the following assumptions are made:

1. Top and bottom boundary elements are rigid enough to neglect their deformation.
2. The behavior of steel plate, strong and weak columns are elastic-perfectly plastic.
3. The Connection of infill plate to boundary elements is strong enough to resist tension field forces.
4. The span to height ratio of the wall dictates the pure shear behavior.

According to the PFI theory proposed by Sabouri [10], the shear capacity of the system (V) is the summation of the shear capacity of the infill plate (V_p), shear capacity of strong column (V_{sc}) and shear capacity of the weak column (V_{wc}):

$$V = V_p + V_{sc} + V_{wc} \tag{1}$$

By considering partially distribution of tension field, shear capacity of infill plate cannot be calculated by considering complete span of the wall. So the shear capacity should be calculated using the effective span that equals with the equivalent span of the fully distributed area. It can be calculated as follows:

$$V_p = \frac{1}{2}\sigma_{ty} t\, b_q \sin(2\alpha) \tag{2}$$

Where σ_{ty}= yielding stress of infill plate, t= infill plate thickness, α= inclination angle of tension filed and bq= effective span of tension field action. The Equation 2 is similar to the equation proposed by Sabouri [10] for shear capacity of the plate and only bq is replaced by b. Because of the unbalance yielding in the participating area, developing an equation based on geometric relations can be imprecise. So it is preferred to present an equation based on numerical study. Consequently, a numerical study in ABAQUS [25] finite element software is carried out by shell elements for shear wall and beam elements for beams and columns. The numerical models cover a various range of span to height ratios, (b/d), and the ratios of plastic moment of weak column to plastic moment of strong column, (M_{pwc}/M_{psc}) are calculated and the parameter c is obtained for each model. The proposed equation for bq based on numerical studies is:

$$b_q = \left[-15.26(b/d)^2 + 32.26(b/d)\right](c/d) + 96.61(b/d) - 14.92 \tag{3}$$

Where, b= span of the infill plate, d= height of the infill plate, c= distance of two plastic hinges in the weak column or the length of weak column's participation area in tension field action that is calculated from Equation 7. The curve of b_q calculation for different ratios of (b/d) and (c/d) from numerical studies is presented in Figure 4.

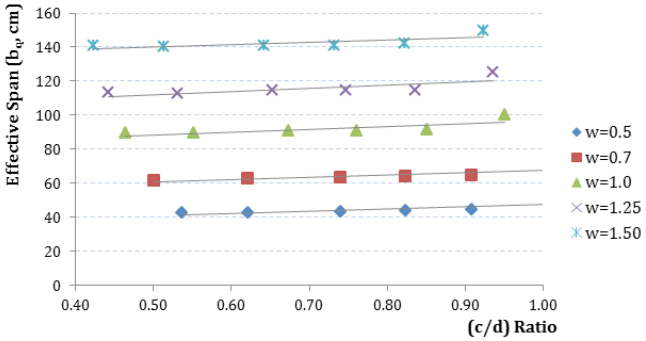

Figure 4. Variation of effective span, b_q, versus (c/d) ratio

Shear displacement of infill plate is obtained by calculating the work conducted by the post-buckled component of the shear forces to the strain energy of the tension field. This leads to:

$$\frac{1}{4}\sigma_{ty} t\, b_q \sin(2\alpha) U_p = \frac{\sigma_{ty}^2}{2E} t\, b_q d \tag{4}$$

Or

$$U_p = \frac{2\sigma_{ty}}{E\sin(2\alpha)} d \tag{5}$$

Where E= modulus of elasticity of infill plate and d= height of the infill plate. Equation 5 is similar to the equation proposed by Roberts and Sabouri [10] for shear displacement of the infill plate. It should be noted that in calculating the strain energy of tension field, the trapezoidal area located above the triangular non-participating area is neglected. As

mentioned above, the parameter c is the participating length of the weak column in load carrying of tension field forces. by assuming a fixed end and guide roller end beam for weak column showed in Figure 5 and by using the principle of energy conservation (i.e., external work=internal work) c is calculated as follows:

$$c = \sqrt{\frac{4M_{pwc}}{\sigma_{ty} t \sin^2 \alpha}} = \frac{2}{\sin \alpha} \sqrt{\frac{M_{pwc}}{\sigma_{ty} t}} \quad (6)$$

In which M_{pwc}= plastic moment of weak column.

According to the PFI theory proposed by Roberts and sabouri [10], the shear capacity of strong and weak column is calculated as follows:

$$V_{sc} = 2M_{psc} / d \quad (7)$$

$$V_{wc} = 2M_{pwc} / c \quad (8)$$

Where M_{psc}= plastic moment of strong column

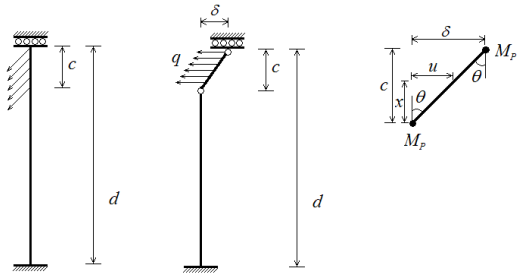

Figure 5. Force diagram in weak column and definition of c parameter

Lateral displacement of strong column top by formation of plastic mechanism is defined as follows:

$$U_{sc} = \frac{M_{psc} d^2}{6EI_{sc}} \quad (9)$$

Where I_{sc}= moment of inertia of strong column. Lateral displacement of weak column top, which is the sum of elastic deformation and plastic deformation arising from formation of plastic mechanism, is defined as follows:

$$U_{wc} = \frac{M_{pwc} c^2}{6E\ I_{wc}} + \frac{M_{pwc}.(d-c).c}{E\ I_{wc}} \quad (10)$$

Where I_{wc}= moment of inertia of weak column. Finally, the shear capacity of plate, strong column, and weak column are calculated by Equations 2, 7 and 8 respectively. The deflection of each component is also calculated by Equations 5, 9 and 10 respectively. By superposing the load-displacement curve of each component, the load-displacement curve of the system can be derived as shown in Figure 6.

A special case of the proposed model is a system in which the weak column properties are equal to the strong ones; this is a common steel plate shear wall with equal columns. Therefore, using c parameter instead of d in the proposed relations, the PFI theory formulation presented by Roberts and Sabouri [10] is reached.

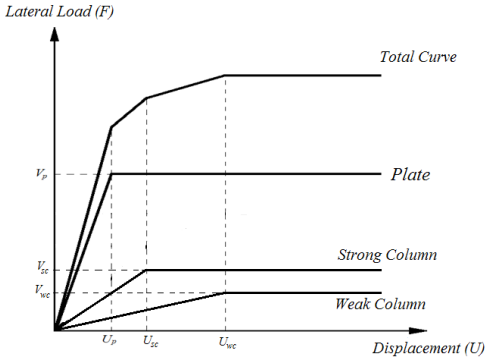

Figure 6. Components of the proposed theoretical model shear load–displacement: frame only, strong column only, weak column only and combined four-linear curve for SPSW with unequal column

3- Inclination angle of tension field

As described earlier, the inclination angle of tension field in SPSW with unequal columns is different from the usual relation used for steel plate shear walls. Therefore, it is necessary to achieve a comprehensive relation for it. In this way, it is referred to the Timler and Kulak [9] works that have been developed based on the principle of least work done by the system. According to the Timler and Kulak investigations, the distribution of tension field is uniform and so the work done by the side columns is the same. However, in an SPSW with unequal columns, distribution of tension field is not uniform and so the work done by the strong and weak columns is different and must be considered separately. One of the basic assumptions in this study is the consideration of high rigidity for top and bottom beam due to pure shear behavior and neglecting of their internal work effect. The procedure of determining the tension field angle will be presented later. It is assumed that the effective components in calculating the work done by the system are: (a) infill plate axial work by considering participating and none-participating area, (b) strong columns axial work, (c) weak columns axial work, (d) strong columns bending work, (e) weak columns bending work. Therefore, the whole work done by the system is as follows:

$$W_{TOTAL} = \frac{V^2 d}{2Etb\sin^2\alpha\cos^2\alpha} - \frac{V^2 d(d-2c+cm)\tan\alpha}{4Etb^2\sin^2\alpha\cos^2\alpha} + \frac{k_{sc}^2 V^2 d}{2EA_{sc}\tan^2\alpha} + \frac{k_{wc}^2 V^2 d}{2EA_{wc}\tan^2\alpha} + \frac{V^2 d^5\tan^2\alpha}{1440EI_{sc}b^2} + \frac{V^2 c^5 u\tan^2\alpha}{1440EI_{wc}b^2} \quad (11)$$

By differentiating Wtotal; with respect to α, and setting (∂Wtotal/$\partial\alpha$) =0, a quantic polynomial with the variable of $\tan\alpha$ is obtained and can be solved by numerical procedures.

$$\frac{dW_{total}}{d\alpha}=0 \quad \Rightarrow$$
$$-3\frac{V^2 d(d-2c+cm)}{4Etb^2}\tan^5\alpha + 2\left(\frac{V^2 d}{2Etb}+\frac{V^2 d^5}{1440EI_{sc}b^2}+\frac{V^2 c^5 u}{1440EI_{wc}b^2}\right)\tan^4\alpha - 2\frac{V^2 d}{2Etb}\tan^3\alpha + \frac{V^2 d(d-2c+cm)}{4Etb^2}\tan\alpha - 2\frac{V^2 d}{2Etb} - 2\frac{k_{sc}^2 V^2 d}{2EA_{sc}} - 2\frac{k_{wc}^2 V^2 d}{2EA_{wc}} = 0 \quad (12)$$

Where d= story height; b= span of the infill plate; c= participation length of tension field on the weak column or the distance of plastic hinges in the weak column. The main parameters affecting the above formula by changing the amount of α are (b/d) and (c/d) ratios. By changing the weak column section properties with respect to strong column, the amount of c parameter will be changed. Similarly, changing the ratio of b/d in the above formula will change α. Figure 7 shows the curve of inclination angle of tension filed versus (c/d) ratio for various ratios of (b/d).

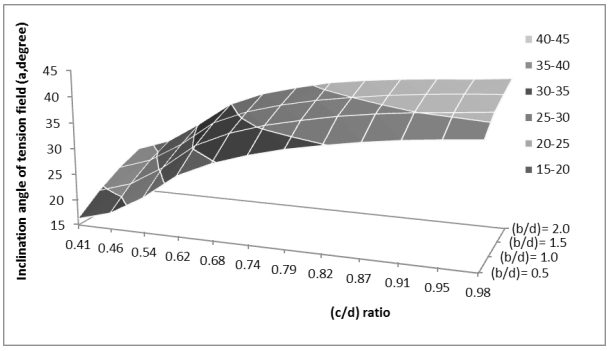

Figure 7. Variation of inclination angle of tension field

In order to simplify the calculation of α and avoid numerical analysis, it is recommended to have a simple equation that is derived from curve fitting in the various ratios of (b/d) and proposed as follows:

$$\alpha = (b/d)(5.054 - 5.741Ln(c/d)) + 29.018Ln(c/d) + 37.725 \quad (13)$$

In Figure 7, data points are related to Equation 12 and the continuing lines are related to Equation 13. It is clear that there is a good agreement between Equation 13 and the values obtained from Equation 12.

4- Experimental study

In order to evaluate the performance of the proposed theoretical relations, an experimental program is designed. In this study, two specimens of steel plate shear walls with unequal columns are loaded under quasi-static cyclic loading. The first specimen named as UC-SPSW1 is an unstiffened steel plate shear wall with one strong and one weak column. The objective of the first test is investigating the behavior of SPSW with unequal columns and verifying the accuracy of proposed theoretical relations. Second specimen named as UC-SPSW2 is an SPSW with the same dimension and properties for strong column but different and weaker properties for weak column. The objective of the second test is to evaluate the possibility of substituting a weak column with a much weaker column accompanied by horizontal and vertical stiffeners. Since the scope of this paper is verifying the accuracy of proposed theoretical relations, therefore the first test is considered extensively.

4- 1- Specification of specimen and test setup

The typical assemblies of the specimen are infill plate, strong column, weak column and top beam. The thickness of the infill plate is considered as 2 mm. centerline distance between side columns is 750 mm and their height is 1000 mm. Strong column, weak column, and top beam are made up of steel plates by welding. The dimensions of strong column flange and the web are 180 × 18 mm and 44 × 8 mm respectively, and the dimensions of weak column flange and the web are 80 × 10 mm and 40 × 5 mm. The dimensions of top beam flange and the web are 200 × 20 mm and 230 × 20 mm respectively. Bottom rigid beam holds the specimen is made of steel plate by welding and connected to the laboratory strong floor by 10 high strength bolts. The geometrical properties of the frame members are presented in Table 1.

Table 1. Definition of member specifications

Member	Width (mm)	Thickness (mm)	Width (mm)	Thickness (mm)
Top Beam	200	20	230	20
Bottom Beam	220	20	230	15
Strong column	180	18	44	10
Weak column	80	10	40	5

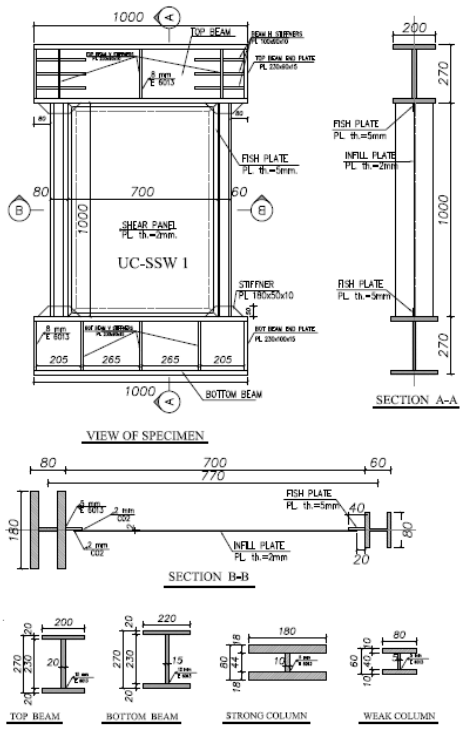

Figure 8. Specification and details of the specimen, beams and column cross sections and welding details

The dimensions of bottom rigid beam flange and the web are 220 × 20 mm and 230 × 15 mm respectively. A 50 × 5 mm strip plate is used as fishplate and the infill plate is lapped over it and is welded continuously to the fishplate. Complete penetration groove welding is used to create full moment connection between top beam to columns and columns base to bottom rigid beam. Fig. 8 shows the specification of specimen, horizontal and vertical cross sections of specimens, dimensions of the columns and top beam, and details of connections and welding. The lateral shear force applied by a slow hydraulic jack to better control the applied displacements. Figure 9 shows the fabricated specimen before test. In order to protect the specimen from lateral displacements and buckling, a pair of guiding beams as lateral restraint is used.

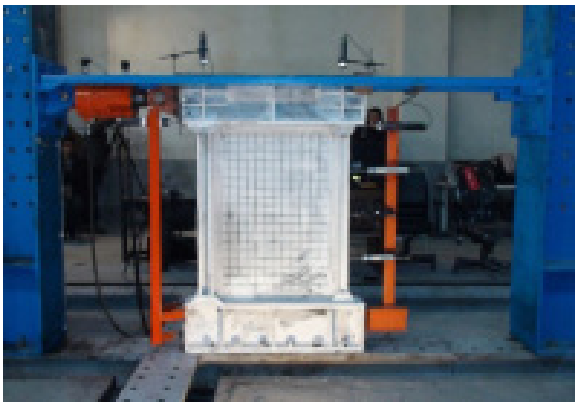

Figure 9. Experimental Specimen before conducting the test

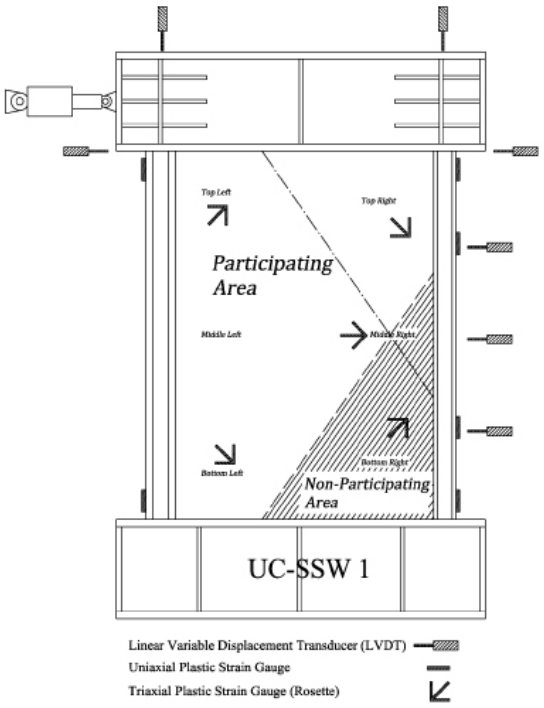

Figure 10 . Instrumentation arrangement and zoning of infill plate

Two pressure transmitters are installed on compression and tension cell of hydraulic jack that measure the applied shear force. In order to convert the obtained pressure from hydraulic jack to force units, the parameters of the jack fabricator are used. Linear variable displacement transducers (LVDTs) are used to measure the displacements of the specimen. Two LVDTs are used to measure the story shear displacements, which are installed at the bottom level of the top beam. Furthermore, LVDTs are also used to measure the deformation of the weak columns, the vertical movements of columns and top beam. At top and bottom levels of strong column as well as top, bottom and two predicted location for plastic hinges in weak column, plastic strain gauges are mounted on exterior flanges to determine the strain. Rosette strain gauges are located at different places on the infill steel plate in order to obtain the principal strains and the maximum shear strains and determining the participating and none-participating areas in tension field action on the infill plate. The locations of the rosettes and plastic strain gauges are determined at probable plastic zones in the elements, based on the preliminary numerical analysis results. In order to have a simple description of the specimen events, a suitable zoning including participating and none-participating areas and positions of the installed rosettes in the infill plate are described. Figure 10 shows the zoning and the locations of the instruments. In order to avoid the errors arising from specimen movement relative to strong floor, all displacement sensors are attached to the specimen at the rigid bottom beam, and so all displacement measuring are relative to the specimen itself. High-strength steel is used for strong column, weak column, beams and infill plate. Tension test is carried out according to the ASTMA370-05 to determine the mechanical properties of the material [17]. A490 high strength bolts are used to connect the bottom rigid beam to the laboratory strong floor.

4- 2- Cyclic loading program

The loading program is applied based on ATC-24 [18] protocol. Before testing, the yielding shear displacement and shear yielding force of infill plate is predicted by proposed theoretical relations and numerical study. According to the protocol, the first and second three cycles of loading are performed respectively by 50 and 75 percent of infill plate yielding shear force. In other words, the elastic cycles should be conducted in force control regime. After determination of the yield point, testing process should be performed in displacement control regime [18]. The test could be stopped when the lateral load dropped below 80% of the maximum load. Figure 11 shows the loading history consists of stepwise increasing deformation cycles, and the number of cycles, which are used, in each loading step.

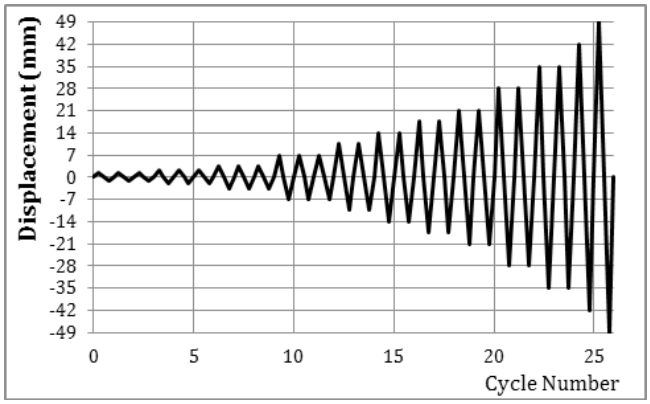

Figure 11. Lateral load history according to ATC24

4- 3- Structural behavior of the specimen by theoretical relations

The structural behavior of the specimen including force-displacement curve, location of plastic hinges in strong and weak columns and inclination angle of tension field are calculated by the proposed relations and a summary of the calculations is presented in Table 2.

4- 4- Test description

Regards to results obtained from theoretical and numerical investigations, yielding force and yielding displacement are estimated. According to ATC-24 loading protocol, 50 percent of estimated yielding force in the first three cycles and 75 percent of estimated yielding force in second three cycles are applied. From 7th cycle, the procedure continued on displacement control regime until initial yielding occurred. In this way, yielding force and yielding displacement in UC-SPSW1 specimen are 267.2 kN and 3.5 mm respectively. Cycles 7, 8 and 9 is continued by δ y (3.5 mm) displacement. In the 7th cycle, the installed rosettes on the middle right zone of the shear panel showed the initial yielding at the story shear displacement of 2.47 mm (0.247 % drift) and story shear force of 243.6 kN. Also in this cycle, the installed rosettes on the bottom right and bottom left zones showed the initial yielding at the story displacement of 3.29 mm (0.329 % drift) and story shear force of 247.2 kN. In the 8th cycle, the exterior flange of weak column yielded at the base in 3.8 mm (0.329 % drift) displacement and the shear force of 252.7 kN. In the end of 9th cycle, global buckling of infill plate is initiated as shown in (Figure 12b). Three cycles of 10, 11 and 12 are continued by (2δ y) displacement. During 10th cycle, rosettes installed on top left and top right of the shear panel showed yielding event at the story shear displacement of 5.26 mm (0.526 % drift) and story shear force of 274.3 kN and also initial buckling of the shear panel occurs.

Table 2. Summary of the proposed theoretical relations and calculations for UC-SPSSW1 specimen

Step	Description	Equation Reference	Calculated Value *
1	Assuming the plate thickness and columns properties		
2	Calculation of inclination angle of tension field	Eq. 19	27.33 deg
3	Calculating c parameter by using step 2 value	Eq. 6	598 mm
4	Calculating b_q value	Eq. 3	596 mm
5	Calculating shear capacity of infill plate V_p	Eq. 2	165.7 kN
6	Calculating shear displacement of infill plate U_p	Eq. 5	4.2 mm
7	Calculating shear capacity of strong column V_{sc}	Eq. 7	119.6 KN
8	Calculating shear displacement of infill plate U_{sc}	Eq. 9	7.5 mm
9	Calculating shear capacity of strong column V_{wc}	Eq. 8	62.6 kg
10	Calculating shear displacement of infill plate U_{wc}	Eq. 10	18.9 mm
11	Calculating shear capacity of entire system	Eq. 1	348.1 KN

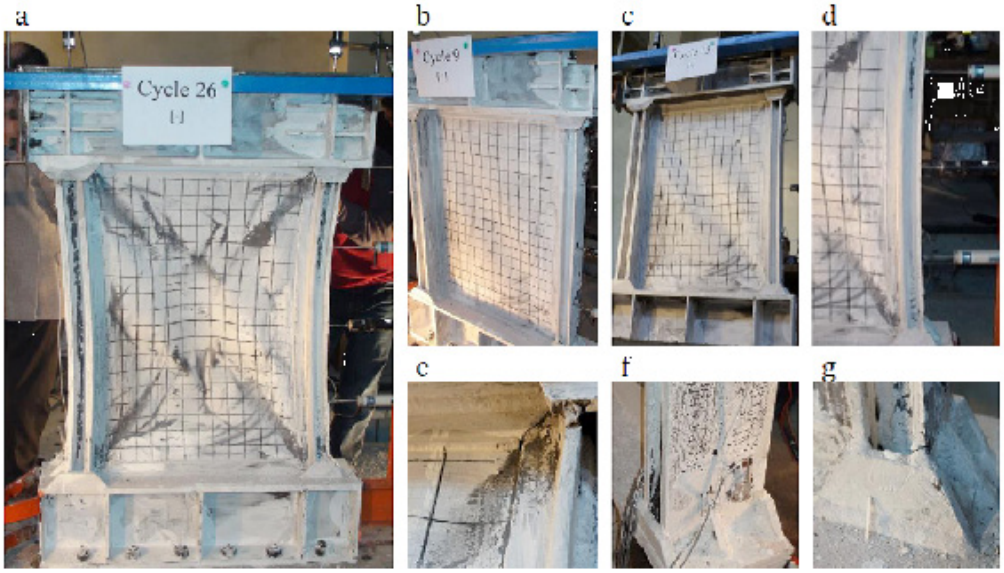

Figure 12. Details of UC-SPSW1 during test, (a) view of the specimen after termination of the test in front view, (b) global buckling initiation of infill plate at cycle 9, (c) clear observation of global buckling at cycle 15, (d) deformed shape and plastic hinges of weak column, (e) cracking and tearing of fish plate in corners of the panel, (f) formation of plastic hinge and crusting of lime coating at the base of strong column, (g) cracking occurred at the base stiffeners of weak column

Two cycles 13 and 14 are continued by displacement of (3 δ y). In 13th cycle, rosettes installed on middle right zone of shear panel showed yielding at the story shear displacement of 7.43 mm (0.743 % drift) and story shear force of 289.1 kN. Also in this cycle, the exterior flange of strong column at the base and top of the column yielded in 8.99 mm (0.899%drift) displacement and 300.7 kN shear force (Figure 12f). In 14th cycle, bottom right zone of shear panel showed yielding on attached rosettes at the story displacement of 10.02 mm (1.002 % drift) and story shear force of 297.6 kN. In this cycle, also small cracking at the top left corner in fishplate welding occurs (Figure 12e). Two cycles 15 and 16 are continued by displacement of (4 δ y). At the end of 16th cycle, the buckling deformation of the infill plate is clearly observed (Figure 12c). In addition, Borders of participated and non-participated area initially created in the shear panel (Figure 13a). Two cycles 17 and 18 are continued by displacement of (5δ y). At the end of 18th cycle, the cracking in fishplate developed to the other corners. Plastic hinges that created in top and bottom of the strong column is expanded to the central parts of the column. Two cycles 19 and 20 are continued by displacement of (6 δ y). During 20th cycle, the buckling deformation of the infill plate is severely established. In addition, the web of the weak column in top, bottom and location of top in span plastic hinge showed crusting of lime coating (Figure 12d). Two cycles 21 and 22 are continued by displacement of (8δ y). At the end of 22nd cycle, a significant cracking occurred at the base stiffeners of weak column (Figure 12g). There is no zipping of infill plate until that time of the testing. Two cycles of 23 and 24 are continued by displacement of (10 δ y). The ultimate shear strength of 364.4 kN is obtained in cycle 24th in 34.9 mm (3.4% drift) displacement. At the end of this cycle, tearing of infill plate at the corners completely observed. Cycles 25 and 26 separately continued by displacement of (12 δ y) and (14 δ y) respectively. Eventually, the test is terminated in cycle 26, in 49 mm (4.9 % drift) displacement and strength of 358.6 kg. The view of the specimen after termination of the test is shown in Figure 12a.

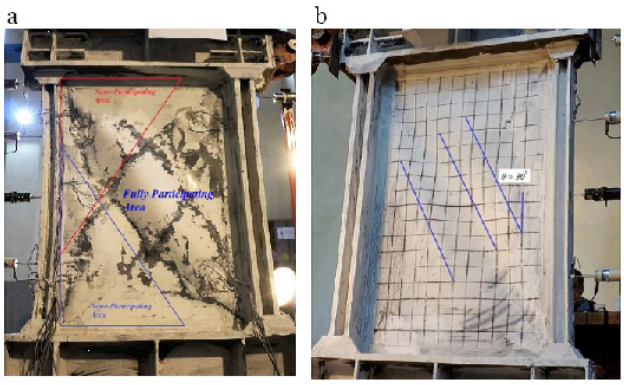

Figure 13. Zoning detail of UC-SPSW1 specimen (a) Definition of participated and non-participated area on the infill plate, (b) inclination angle of tension field on the specimen

4- 5- Test results and discussion

As mentioned in test description, the triangular areas in top and bottom of the infill plate near the weak column are not participated in tension field as predicted in theoretical assumptions and have not significant contribution in energy dissipation because of no deformation occurrences in these areas. As shown in Figure 13a the crusting of lime coating in these areas is not observed. An extensive area in the center of infill plate in diagonal direction globally buckled and have significant in energy dissipation of the system. Hysteresis curve is one of the main indexes in performance of the system that is created by applying the cyclic loads to lateral

load resisting system as shown in Figure 14 for the UC-spsw1 specimen.

According to Figure 14 it can be said that although all parts

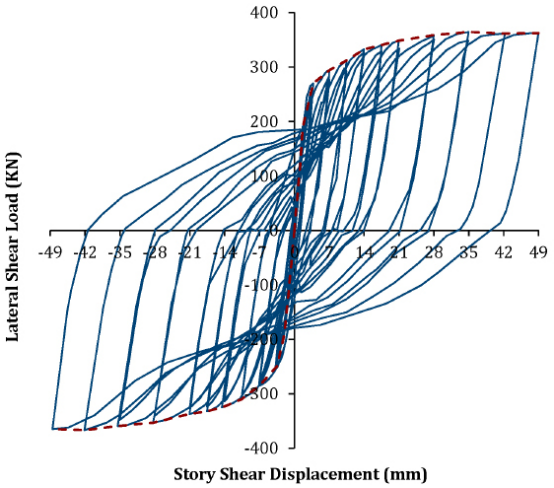

Figure 14. Hysteresis and envelope curve of UC-SPSW1 specimen

of the infill plate are not participated in the energy dissipation of the system, however, the specimen has spindle shape and stable hysteresis loops. In order to investigate the occurrence and position of plastic hinges in the main column, the strain history of the two strain gauges attached to the top and bottom of the main column are recorded as shown in Figure 15.

According to Figure 15, it is observed that the strain in

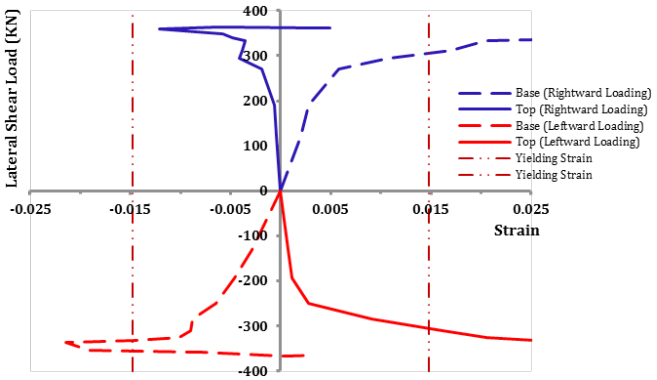

Figure 15. Strain history in probable position of the strong column in top and bottom in loading and unloading regime

plastic hinges in top and bottom of the strong column exceed or are near to the yield strain. This means that plastic hinges have been formed in the predicted locations of the strong column. In addition, the strain history of the four strain gauges attached to the predicted locations of the plastic hinges in weak column are shown in Figure 16.

According to Figure 16, the strain situation of the predicted locations in both loading and unloading regimes exceeds from yielding strain

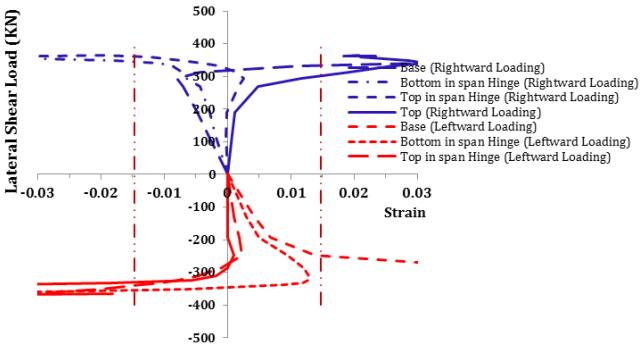

Figure 16. Strain history in probable position of the weak column in loading and unloading regime

5- Comparison of Theoretical and Experimental Results

In order to verify the results of experimental tests with theoretical results, the load-displacement curve obtained from theoretical relations is compared with hysteresis envelope curve of the test shown in Figure 17.

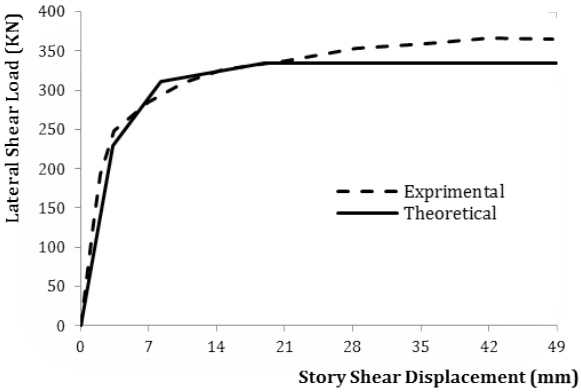

Figure 17. Four-linear analytical load-displacement curve and hysteresis envelope curve of specimen

The initial stiffness of the theoretical curve is coincident with experimental curve. The yielding force and displacement of the system that is equal to the yielding force and displacement of the infill plate are in coincides to the initial yielding force and displacement of the test results. The shear displacement calculated by Equation 5 is 3.4 mm according to Table 1 and the shear displacement recorded in the test is 3.5 mm. The ultimate lateral shear load calculated by Equation 1 is 348.1 kN and the ultimate lateral shear load recorded in the test is 358.5 kN. The difference between ultimate shearloads is about 10% that is caused by the elastic-perfect plastic assumption used in theoretical relations. Referring to Figure 13a, the two triangular non-participating areas are similar to the predicted non-participating area shown in Figure 10 and basic concepts of theoretical relations in Figure 3. This means that the basic concepts used in developing the theoretical relations are good and acceptable. The inclination angle of the tension field calculated by Equation 19 is about 27 degree and the inclination angle of tension field estimated in test specimen is about 30 degree that is shown in Figure 13b. Therefore, there is a good agreement in the inclination angle of tension field in theoretical and experimental results.

In order to further verification of the proposed theoretical equations, a series of finite element modelling based on variation of span to height ratio, ω= b/d which is tabulated in Table 3, is carried out and the results are compared with the results of theoretical equations. For simplicity in changing parameters the panel height is defined as a constant parameter and equal to 1000 mm and the changing of the models done by changing the span values. The structural properties of models such as strong column, weak column, top beam and infill plate and material properties are the same for each 6 models.

Table 3. Configuration of numerical models

	case1	case2	case3	case4	case5	case6
ω	0.50	0.70	1.00	1.25	1.50	1.70

Load–Displacement curves from numerical analysis together with curves from theoretical relations for models is compared and shown in Figure 18.

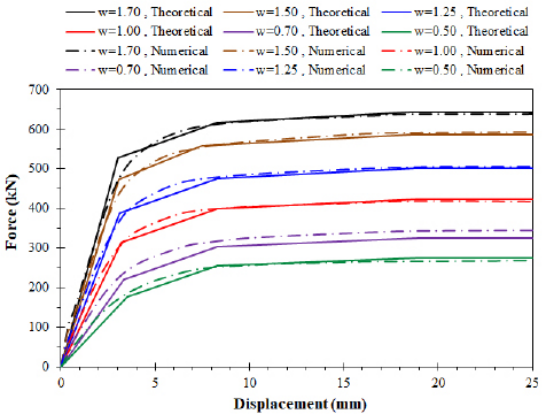

Figure 18. Comparison of numerical and analytical load-displacement curve for models

As it can be seen from Figure 18, the results of the proposed theoretical equations and numerical simulations are in good agreement in initial stiffness, yielding point and ultimate strength.

6- Conclusion

In this paper, the behavior of a steel plate shear wall with unequal column because of its different action is theoretically and experimentally investigated. Theoretical relations proposed for predicting the shear capacity of the system based on the PFI method also relations for defining the inclination angle of tension field due to different action of tension field in these systems. In continue, an experimental study is performed for verifying the accuracy of proposed relations. By surveying the results of experimental and theoretical works, the following conclusions can be made:

1. The load-displacement curve obtained from theoretical relations has good agreement with the load-displacement curve of the experimental work. This shows accuracy and conformity of the shear capacity relations.
2. Predicted locations to formation of plastic hinges on the strong and weak columns by theoretical relations are near matches to the location of plastic hinges that took place in experimental study.
3. The predicted relation for inclination angle of tension field is almost the same as the inclination angle observed in experimental work.
4. The predicted areas named as participating and none-participating areas that used in developing the theoretical relations are clearly observed in the experimental study and show that the basic assumptions that theoretical relations developed based on them are correct and inclusive.
5. Experimental results show that the specimen has spindle shape and stable hysteresis loops although one of the columns is weaker than the other one. If the weak column participates properly in tension field action of the shear wall, the system has suitable behavior and acceptable energy dissipation.

In addition to experimental test, finite element modelling is used to examine the accuracy of the proposed equations. 6 different span to height ratios are considered and the corresponding numerical models are developed. The results of these models are compared with the theoretical calculations and good agreement is achieved. Although further numerical investigations will be to provide higher assurance.

References

[1] P. Timler, C.E. Ventura, H. Prion, R. Anjam, Experimental and analytical studies of steel plate shear walls as applied to the design of tall buildings, The Structural Design of Tall Buildings, 7(3) (1998) 233-249.

[2] H. Valizadeh, M. Sheidaii, H. Showkati, Experimental investigation on cyclic behavior of perforated steel plate shear walls, Journal of Constructional Steel Research, 70 (2012) 308-316.

[3] S. Sabouri-Ghomi, S. Mamazizi, Experimental investigation on stiffened steel plate shear walls with two rectangular openings, Thin-Walled Structures, 86 (2015) 56-66.

[4] H. Wagner, Flat sheet metal girders with very thin metal webs, Part I -General theories and assumption., NACA Tech. Memo, (1931).

[5] K. Basler, Strength of Plate Girders in Shear, Journal of the Structural Division, 87(7) (1961) 151-180.

[6] D.M. Porter, K.C. Rockey, H.R. Evans, The collapse behavior of plate girders loaded in shear, The Structural Engineer, 53(8) (1975) 314-325.

[7] Y. Takahashi, T. Takeda, Y. Takemoto, M. Takagai, Experimental study on thin steel shear walls and particular steel bracing under alternating horizontal loading, in: Proceedings of the IABSE symposium, resistance and ultimate deformability of structures acted on by well-defined repeated loads, Lisbon, Portugal, 1973, pp. 185–191.

[8] L.J. Thorburn, G.L. Kulak, C.J. Montgomery, Analysis and design of steel shear wall system, No. 107, Dept. of Civil Engineering, Univ. of Alberta, Alberta, Canada, 1983.

[9] P.A. Timler, G.L. Kulak, Experimental study of steel plate shear walls, No. 114, Dept. of Civil Engineering, Univ. of Alberta, Alberta, Canada, 1983.

[10] T.M. Roberts, S.S. Ghomi, Hysteretic characteristics of

unstiffened plate shear panels, Thin-Walled Structures, 12(2) (1991) 145-162.

[11] S.-G. S., Lateral Load Resisting An Introduction To Steel Plate Shear Walls, Anghizeh Publishing Co., Tehran, Iran, 2002.

[12] S. Sabouri-Ghomi, C.E. Ventura, M.H. Kharrazi, Shear Analysis and Design of Ductile Steel Plate Walls, Journal of Structural Engineering, 131(6) (2005) 878-889.

[13] T.M. Roberts, S. Sabouri-Ghomi, Hysteretic characteristics of unstiffened perforated steel plate shear panels, Thin-Walled Structures, 14(2) (1992) 139-151.

[14] J. Berman, M. Bruneau, Plastic Analysis and Design of Steel Plate Shear Walls, Journal of Structural Engineering, 129(11) (2003) 1448-1456.

[15] D. Vian, M. Bruneau, Testing of special LYS steel plate shear walls, in: Proceedings of the 13th world conference on earthquake engineering, Vancouver, Canada, 2004.

[16] J. Kee Paik, Ultimate strength of perforated steel plates under combined biaxial compression and edge shear loads, Thin-Walled Structures, 46(2) (2008) 207-213.

[17] R. Purba, M. Bruneau, Finite-Element Investigation and Design Recommendations for Perforated Steel Plate Shear Walls, Journal of Structural Engineering, 135(11) (2009) 1367-1376.

[18] I.-R. Choi, H.-G. Park, Steel Plate Shear Walls with Various Infill Plate Designs, Journal of Structural Engineering, 135(7) (2009) 785-796.

[19] S. Sabouri-Ghomi, S.R.A. Sajjadi, Experimental and theoretical studies of steel shear walls with and without stiffeners, Journal of Constructional Steel Research, 75 (2012) 152-159.

[20] S.R.A. Sajjadi, Behavior of steel plate shear walls opening, PhD dissertation, KNT Univ. of Technology, Tehran, Iran, 2009.

[21] S.A.A. Hosseinzadeh, M. Tehranizadeh, Introduction of stiffened large rectangular openings in steel plate shear walls, Journal of Constructional Steel Research, 77 (2012) 180-192.

[22] R. Purba, M. Bruneau, Experimental investigation of steel plate shear walls with in-span plastification along horizontal boundary elements, Engineering Structures, 97 (2015) 68-79.

[23] M. Wang, W. Yang, Y. Shi, J. Xu, Seismic behaviors of steel plate shear wall structures with construction details and materials, Journal of Constructional Steel Research, 107 (2015) 194-210.

[24] M. Kurata, R.T. Leon, R. DesRoches, M. Nakashima, Steel plate shear wall with tension-bracing for seismic rehabilitation of steel frames, Journal of Constructional Steel Research, 71 (2012) 92-103.

[25] M. Smith, ABAQUS/Standard User's Manual, Version 6.14, Simulia, Providence, RI, 2014.

[26] ASTM, ASTM A370 - 05, Standard Test Methods and Definitions for Mechanical Testing of Steel Products, in, 2005.

[27] ATC-24, Guidelines for cyclic seismic testing of components of steel structures, in, Applied Technology Council, Redwood City, CA, 1992.

Appendix A: list of symbols

symbol	Description
α	Inclination angle of tension field
c	Participating length of weak column in tension field action
b_q	Effective span of the wall
V_p	Shear capacity of infill plate
U_p	Shear displacement of infill plate
V_{sc}	Shear capacity of strong column
U_{sc}	Shear displacement of infill plate
V_{wc}	Shear capacity of strong column
U_{wc}	Shear displacement of infill plate
V	Shear capacity of entire system

Appendix B: comparison of experimental results with theoretical predictions for key parameters

Parameter	Experimental	Calculated Value *
α	30 deg	27.33 deg
c	490 mm	598 mm
b_q	510 mm	596 mm
V_p	170 KN	165.7 KN
U_p	4 mm	4.2 mm
V_{sc}	125 KN	119.6 KN
U_{sc}	9.5 mm	7.5 mm
V_{wc}	65 KN	62.6 KN
U_{wc}	21 mm	18.9 mm
V	350 KN	348.1 KN

Please cite this article using:
P. Mousavi Qieh-Qeshlaghi, S. Sabouri-Ghomi, Theoretical and Experimental Study on Steel Plate Shear Wall with Unequal Columns, *AUT J. Civil Eng*, 2(1) (2018) 103-114.
DOI: 10.22060/ajce.2017.12425.5213